cosmetics

MDPI

Article

Post-Electrospinning Surface Functionalization of PCL Nanofibrous Membranes with Sisal Extracts: Extract-Dependent Cytocompatibility and Bioactivity

Felipe Romici Zane Lordelo Nogueira [1,*], Julia Amanda Rodrigues Fracasso [2], Luisa Taynara Silvério da Costa [2], Wellington Ricardo Pereira Martins [2], Amanda Letícia Santos Costa [2], Ligia Maria Manzine Costa [3] and Lucinéia dos Santos [2]

[1] Faculty of Pharmaceutical Sciences, São Paulo State University (UNESP), Araraquara 14800-903, Brazil
[2] Department of Biotechnology, School of Sciences and Languages, São Paulo State University (UNESP), Assis 19806-900, Brazil; j.fracasso@unesp.br (J.A.R.F.); luisa.silverio@unesp.br (L.T.S.d.C.); wellington.martins@unesp.br (W.R.P.M.); als.costa@unesp.br (A.L.S.C.); lucineia.santos@unesp.br (L.d.S.)
[3] Department of Physics and Chemistry, Faculty of Engineering, São Paulo State University (UNESP), Ilha Solteira 15385-000, Brazil; ligia.manzine@unesp.br
* Correspondence: felipe.lordelo@unesp.br; Tel.: +55-11-99933-2620

Abstract

Chronic wounds are frequently associated with persistent inflammation, motivating the development of biofunctional materials capable of modulating cellular responses. In this proof-of-concept study, electrospun poly(ε-caprolactone) (PCL) nanomembranes were surface-functionalized by post-electrospinning drop coating with extracts derived from *Agave sisalana* agroindustrial residue obtained through two distinct routes: a saponin-rich fraction (EDP) and an acid-hydrolyzed sapogenin-enriched fraction (EAH). The study aimed to investigate how the extract phytochemical profile influences cytocompatibility and bioactivity when incorporated onto electrospun platforms. Phytochemical analysis revealed high total saponin content in EDP (33.83 ± 2.93 g/100 g) and significant sapogenin content in EAH (11.56 ± 0.60 g/100 g). SEM and FTIR-ATR analyses confirmed preservation of the fibrous architecture and polymer backbone, indicating predominantly physical surface incorporation. Biological evaluation demonstrated extract-dependent responses: PCL+EDP 5% exhibited marked cytotoxicity, consistent with the known membrane-disruptive properties of glycosylated saponins, whereas PCL+EAH 5% maintained high cell viability and showed anti-inflammatory activity (75% inhibition of phagocytosis; 56% protection against hemolysis) along with enhanced fibroblast migration (100% wound closure at 72 h). These findings highlight the critical role of extract chemical composition in determining the biological performance of surface-functionalized nanofibrous systems and support sapogenin-enriched fractions as safer bioactive modifiers for electrospun biomaterial platforms.

Keywords: electrospinning; poly(ε-caprolactone); nanofibrous membranes; surface functionalization; *Agave sisalana*; saponins; wound healing; cytotoxicity; anti-inflammatory activity; scratch assay

Academic Editor: Eduardo Ricci, Junior

Received: 2 February 2026
Revised: 14 March 2026
Accepted: 18 March 2026
Published: 23 March 2026

1. Introduction

Chronic wounds such as diabetic foot ulcers, pressure ulcers, and vascular lesions represent a major public health burden due to their high prevalence and difficult management.

Globally, more than 20 million people are estimated to be affected by chronic wounds, which often require long-term care and present an increased risk of infection [1]. These persistent lesions prolong healing time and raise healthcare costs, reinforcing the need for more effective and affordable therapeutic approaches. In this context, advanced dressings have gained prominence because they provide a moist environment favorable to tissue regeneration and frequently incorporate bioactive agents that support the healing process.

In recent decades, nanotechnology applied to biomedicine has emerged as a promising strategy for the development of smart wound dressings [2]. In particular, electrospinning enables the fabrication of polymeric nanofiber mats with high surface area, elevated porosity, and a three-dimensional architecture similar to the extracellular matrix, which are beneficial features for cell adhesion and gas exchange in wound care applications [3]. These nanomembranes can function both as bioabsorbable scaffolds and as carriers for the controlled release of therapeutic substances [3]. Among the polymers commonly employed, poly(ε-caprolactone) (PCL) stands out because of its biocompatibility, slow biodegradation, and favorable mechanical properties [3]. Electrospun PCL nanofiber mats have already demonstrated success as wound dressings, including systems incorporating bioactive additives such as silver nanoparticles, pharmaceuticals, and natural compounds [3].

At the same time, there is growing interest in the use of natural products with pharmacological activity in wound care applications. Propolis, for example, has been incorporated into PCL nanofibers to exploit its antimicrobial, antioxidant, anti-inflammatory, and wound-healing properties [3]. In the present study, saponins derived from sisal (*Agave sisalana*), a plant species abundant in Brazil, are proposed as bioactive agents for advanced wound dressings. Brazil is the world's largest producer of sisal, generating thousands of tons of residue annually from the leaf-defibering process, known as mucilage, which corresponds to approximately 95% of the leaf mass [4]. Traditionally, sisal juice, which is the liquid fraction of this mucilage, has been used in folk medicine as a topical antiseptic and anti-inflammatory agent [4]. However, this agroindustrial residue remains scientifically underexplored.

Recent studies have demonstrated that extracts obtained from sisal juice are rich in steroidal saponins and their aglycones, referred to as sapogenins, which correspond to the non-glycosylated steroidal moieties released through saponin hydrolysis [5]. The major sapogenins identified in sisal include hecogenin and tigogenin, which are steroidal compounds capable of modulating inflammatory responses in a manner comparable to corticosteroids [5]. Indeed, hydrolyzed sisal extracts have shown pronounced anti-inflammatory activity in experimental models, significantly inhibiting inflammatory edema. At a dose of 50 mg/kg, a reduction of approximately 64% in edema was observed, exceeding the effect of the reference anti-inflammatory drug indomethacin [5]. In addition, these extracts exhibited low acute toxicity in preclinical studies, with no mortality or adverse clinical signs reported in rodents at oral doses of up to 1000 mg/kg [5]. Analgesic effects and the absence of significant cytotoxicity have also been demonstrated in vitro using human cell models [4]. Furthermore, saponins are known to display antimicrobial activity by acting as surfactants that disrupt microbial cell membranes, thereby contributing to wound asepsis. Although several studies have investigated plant-extract-loaded electrospun systems for wound-related applications, limited attention has been given to how distinct phytochemical fractions derived from the same biomass influence cytocompatibility and immunomodulatory behavior when applied via post-electrospinning surface functionalization. In particular, comparative analyses between glycosylated saponin-rich fractions and their hydrolyzed sapogenin-enriched counterparts remain scarce, despite their known differences in polarity, membrane interaction, and biological activity.

In this context, the present study proposes a proof-of-concept evaluation of electrospun poly(ε-caprolactone) nanomembranes surface-functionalized with two chemically distinct extracts obtained from *Agave sisalana* agroindustrial residue. Rather than focusing on full translational validation of a wound dressing, the objective was to investigate how the extract's phytochemical profile modulates physicochemical integrity and in vitro biological responses, including cytocompatibility, inflammatory modulation, and fibroblast migration. By comparatively assessing saponin-rich (EDP) and sapogenin-enriched (EAH) fractions, this work aims to elucidate the role of extract chemical composition in determining the biological performance of functionalized nanofibrous platforms, while simultaneously exploring a sustainable strategy for biomass valorization. To the best of our knowledge, this is among the first studies to directly compare saponin-rich and sapogenin-enriched fractions derived from the same biomass as post-electrospinning surface modifiers and systematically relate their chemical profile to cytocompatibility and immunomodulatory behavior.

To situate the present work within the current landscape of botanical functionalization of electrospun PCL, most prior studies rely on bulk blending of plant extracts into the spinning solution or on coaxial strategies, which can alter solution rheology, affect spinnability, and confound whether bioactivity arises from matrix modification or surface availability of phytochemicals. In contrast, comparative studies that intentionally pair chemically distinct fractions derived from the same biomass—here, a glycosylated saponin-rich fraction (EDP) versus a sapogenin-enriched hydrolysate (EAH)—and apply them via a post-electrospinning surface deposition route remain scarce. Accordingly, our specific contribution is a head-to-head proof-of-concept comparison of fraction-dependent bioactivity under a surface-functionalization paradigm designed to preserve the PCL backbone and fiber morphology, while enabling mechanistically interpretable biological outcomes (cytocompatibility versus membrane-disruptive cytotoxicity).

2. Materials and Methods

2.1. Plant Material

Sisal mucilage from *Agave sisalana* corresponds to the residue generated during the leaf defibering process used to obtain hard fibers. The mucilage, composed of solid and liquid fractions, was obtained from local producers in the municipality of Valente, Bahia, Brazil, at latitude −11.4133 and longitude −39.4653. The species under study was taxonomically identified as *Agave sisalana* at the Assisense Herbarium of São Paulo State University (UNESP), Assis, São Paulo, Brazil, where a voucher specimen was deposited under accession number 2597.

2.2. Preparation of Sisal Residue Extracts

Two extracts derived from the juice of *Agave sisalana* mucilage were prepared: (i) the extract of the dry precipitate (EDP), obtained from sisal juice, which corresponds to the liquid fraction produced during mucilage pressing for saponin extraction, and (ii) an extract obtained by acid hydrolysis of sisal juice (EAH), aimed at promoting saponin hydrolysis and releasing sapogenins. The extraction routes are schematically illustrated in Figure 1.

For EDP preparation, sisal juice was subjected to centrifugation at 4000 rpm for 20 min at 4 °C to obtain the precipitate. The recovered precipitated material was dried in a rotary oven at 36 °C. For application in the nanomembranes, EDP was resuspended in a 70% (*v*/*v*) hydroalcoholic solution to final concentrations of 1% and 5% (*w*/*v*).

For EAH preparation, sisal juice was acidified to pH 0.4–0.8 using concentrated hydrochloric acid, transferred to hermetically sealed containers, and heated at 120 °C for 150 min to promote acid hydrolysis of saponins. After cooling, the sample was centrifuged at 4000× *g* for 10 min. The precipitate was recovered, washed, and dried to constant mass. The dried

material was then resuspended in a 70% (*v*/*v*) hydroalcoholic solution to final concentrations of 1% and 5% (*w*/*v*). Both extracts were stored in amber glass bottles at 4 °C until use.

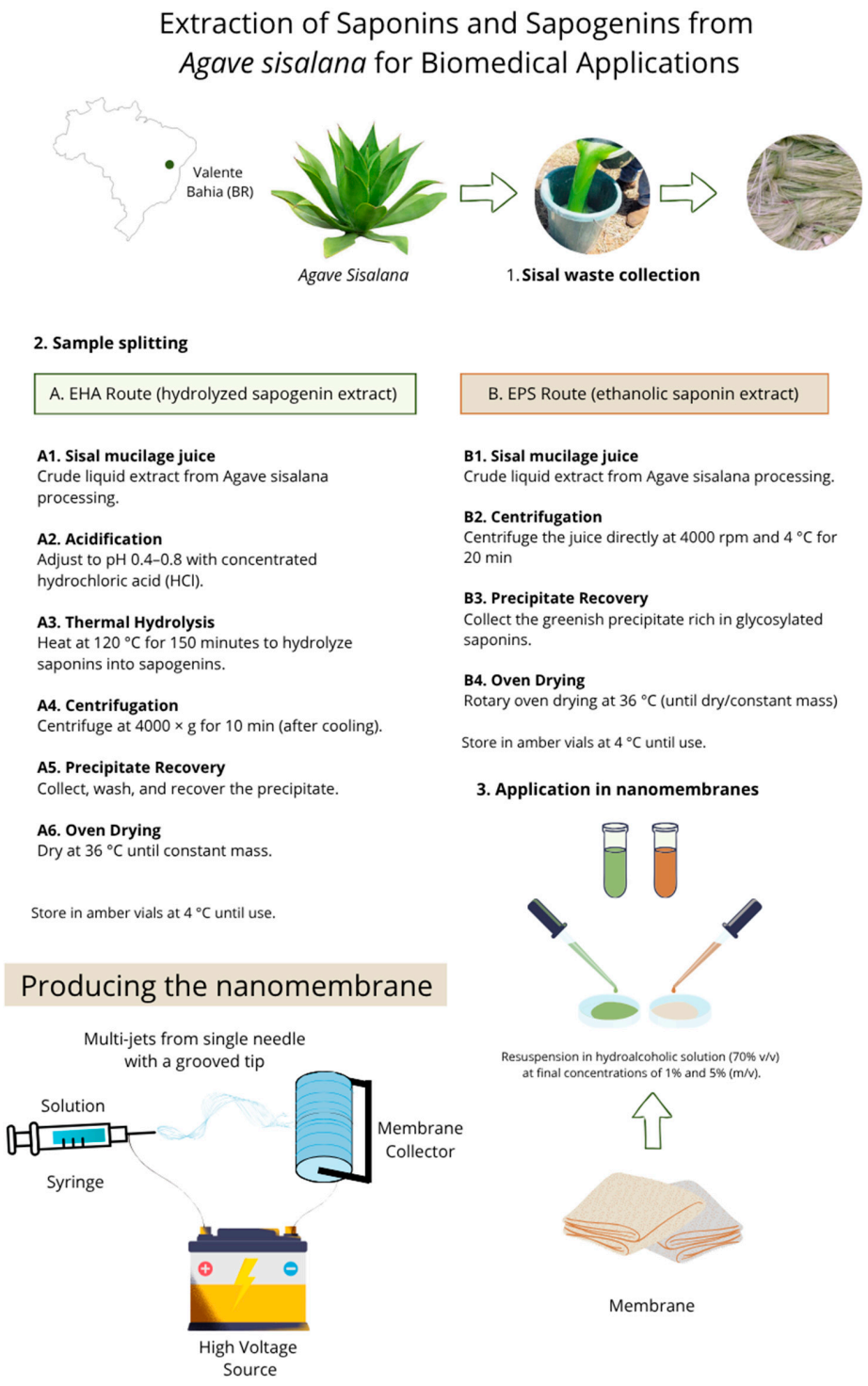

Figure 1. Thematic flowchart illustrating the extraction routes of saponins and sapogenins from *Agave sisalana* and their subsequent application in electrospun PCL nanomembranes. Sisal agroindustrial residues collected in Valente, Bahia (Brazil), were processed and divided into two routes: (A) acid-hydrolyzed extract (EAH), involving juice acidification, thermal hydrolysis, centrifugation, precipitate recovery, and drying to obtain sapogenin-enriched fractions; and (B) extract of the dry precipitate (EDP), based on centrifugation, recovery of glycosylated saponin-rich precipitate, and drying. The resulting extracts were incorporated by surface impregnation into electrospun poly(ε-caprolactone) (PCL) nanomembranes produced using a single-needle electrospinning system, yielding biofunctional membranes for biomedical applications.

2.3. Quantification of Saponins (EDP) and Sapogenins (EAH)

2.3.1. Spectrophotometric Quantification of Saponins in EDP

The presence and quantification of saponins in EDP were evaluated using a colorimetric method with UV-Vis spectrophotometric detection, following protocols described in the literature with minor adaptations. Saponin content was measured in test tubes. An aliquot of 0.25 mL of EDP extract at concentrations of 75, 100, 200, and 400 µg/mL was mixed with 0.25 mL of freshly prepared 10% (*w*/*v*) vanillin solution and 2.5 mL of 72% sulfuric acid, added under cold conditions. The reaction mixture was heated in a water bath at 60 °C for 10 min and subsequently cooled to room temperature. Absorbance was measured at a wavelength of 544 nm using a UV-Vis spectrophotometer.

Quillaja saponin (Sigma-Aldrich, CAS No. 8047-15-2, Burlington, MA, USA) was used as the reference standard. The results for the isolated extracts were expressed as grams of total saponins per 100 g of dry extract [6,7].

2.3.2. Spectrophotometric Quantification of Sapogenins in EAH

Sapogenin quantification in the extract obtained by acid hydrolysis (EAH) was performed using the p-anisaldehyde–H_2SO_4 colorimetric method in ethyl acetate, adapted from Baccou, Lambert, and Sauvaire (1977), with spectrophotometric detection at 430 nm [8]. Two reagent solutions were prepared: Solution A, consisting of p-anisaldehyde in ethyl acetate at 5%, and Solution B, consisting of sulfuric acid in ethyl acetate at a 50:50 (*v*/*v*) ratio.

For each 10 mL test tube, 2.0 mL of diluted sample at concentrations of 75, 100, 200, and 400 µg/mL were mixed with 1.0 mL of Solution A and 1.0 mL of Solution B. The reaction mixtures were incubated at 60 ± 1 °C for 10 min and then cooled to room temperature. Absorbance was measured at 430 nm using a UV-Vis spectrophotometer.

Quantification was performed using a calibration curve constructed with diosgenin standard solutions, and the results were expressed as diosgenin equivalents, in grams per 100 g of dry extract (g/100 g).

2.4. Development of Nanomembranes

Poly(ε-caprolactone) (PCL; Sigma-Aldrich, product 440744, 250 g; average Mn = 80,000 g/mol, melting temperature 58–60 °C; supplier-reported Mw/Mn < 2) nanomembranes were produced by electrospinning using PCL solutions prepared in a binary solvent mixture of chloroform and methanol (4:1, *v*/*v*) at a concentration of 9% (*w*/*w*). The solutions were magnetically stirred for approximately 6 h until complete homogenization [3,9]. The polymer solution was then transferred to a 20 mL glass syringe fitted with a metallic needle with an internal diameter of 0.8 mm and electrospun under an applied voltage of 17 kV. The needle-to-collector distance was set to 12 cm, and a rotating metallic collector operating at approximately 15 rpm was used. Electrospinning was performed at a controlled temperature of 25 ± 2 °C and relative humidity of approximately 50% [3,6].

The solution feed rate was gravity-controlled, with 20 mL of solution deposited per sample, resulting in continuous PCL nanofibrous mats with approximate dimensions of 10 × 10 cm. After deposition, the PCL mats were dried in an oven at 35 °C for 36 h and removed only after completion of the drying period.

Subsequently, post-electrospinning surface functionalization was carried out by drop coating. Hydroethanolic solutions containing EDP or EAH at concentrations of 1% and 5% (*w*/*v*) in 70% (*v*/*v*) ethanol were applied in individual compartments to prevent cross-contamination. This surface functionalization strategy was adopted to promote deposition and adsorption of bioactive compounds without altering the electrospinning process [9]. The samples were then dried under controlled conditions and coded as follows: PCL

(control), PCL+EDP-1%, PCL+EDP-5%, PCL+EAH-1%, and PCL+EAH-5%. The visual appearance of the functionalized membranes and the experimental setup used for surface impregnation are shown in Figure 2.

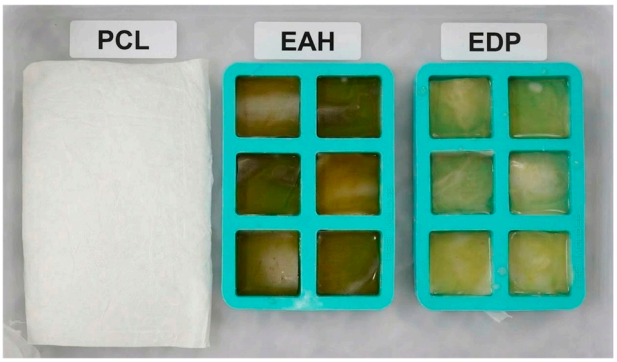

Figure 2. Application of *Agave sisalana* plant extracts to PCL nanomembranes. A PCL nanomembrane is shown alongside membranes placed in individual compartments and impregnated with 70% ethanolic solutions containing acid-hydrolyzed extract (EAH 5%) and saponin ethanolic extract (EDP 5%), at concentrations of 1% and 5%. The compartmentalized mold consists of 6 individual compartments, each measuring 2.5 × 2.5 cm. Each compartment corresponds to a PCL nanomembrane exposed to a specific extract type and concentration. A clear color difference is observed after impregnation: EDP-treated membranes exhibit a greenish hue, whereas EAH-treated membranes show a brownish coloration, reflecting differences in extract composition and chemical profile.

2.5. Scanning Electron Microscopy

The surface morphology of nanomembranes containing 1% and 5% extracts was evaluated by scanning electron microscopy (SEM). Samples with approximate dimensions of 5 × 5 mm were mounted on aluminum stubs using conductive carbon tape and, to minimize electrostatic charging, were sputter-coated with a thin conductive gold layer. Micrographs were acquired under high-vacuum conditions using a secondary electron detector, with an accelerating voltage of 5 kV and magnifications ranging from 1000× to 5000×.

Fiber diameters were quantified from the micrographs using ImageJ Version 1.54p software after calibration with the scale bar. For each experimental condition, multiple randomly selected fields were analyzed, and measurements of 100 fibers were performed to ensure robust estimation. Results were expressed as mean ± standard deviation [9,10].

2.6. Fourier Transform Infrared Spectroscopy

The chemical and structural characterization of the nanomembranes, including control PCL and PCL after surface impregnation with EDP or EAH, was performed by Fourier transform infrared spectroscopy (FTIR) in attenuated total reflectance (ATR) mode using a Bruker ALPHA II spectrometer equipped with a diamond crystal. For each sample, spectra were collected with 32 accumulated scans over the range of 4000 to 400 cm^{-1} at a resolution of 4 cm^{-1}, following background acquisition under identical instrumental conditions. Samples were analyzed directly on the ATR crystal without additional preparation, ensuring uniform contact with the accessory.

Band assignments were performed by comparison with literature data, focusing primarily on characteristic vibrational modes of PCL and *Agave sisalana* constituents, including glycosylated saponins in EDP and more apolar sapogenins in EAH. This analysis aimed to verify the presence and chemical compatibility of the extracts on the membrane surface and to identify potential spectral profile changes after impregnation [4,5,11].

2.7. Cytotoxicity Assay by the MTT Method

Normal mouse fibroblasts (NIH/3T3 cell line, TCC CRL®-1658.2™) were cultured in tissue culture-treated flasks using high-glucose DMEM® medium (Sigma, Cajamar, São Paulo, Brazil) supplemented with 1% penicillin and incubated at 37 °C in a humidified atmosphere containing 5% CO_2. The cell suspension was counted using a Neubauer chamber and diluted to obtain a concentration of 250,000 cells per mL. Subsequently, 80 µL of the cell suspension was seeded into 96-well ELISA plates and incubated overnight.

After incubation, 200 µL of eluates was added to the cells, and the plates were incubated for 24, 48, and 72 h. The eluates were obtained by incubating nanomembrane fragments, including PCL, PCL+EAH 5%, and PCL+EDP 5%, in supplemented high-glucose DMEM at a surface-to-volume ratio of 3 cm^2/mL at 37 °C for 24 h, followed by filtration. After the respective incubation periods, the supernatant was removed, and 100 µL of MTT solution (CAS No. 298-93-1, Sigma-Aldrich, Cajamar, São Paulo, Brazil; 5 mg of MTT per 1 mL of PBS) was added and incubated for 4 h.

Following incubation, the supernatant was removed, and 100 µL of sterile dimethyl sulfoxide (DMSO) was added to solubilize the formazan crystals, followed by an additional incubation for 10 min. The solution was homogenized, and absorbance was measured using an ELISA spectrophotometer at 540 nm.

2.8. Pharmacological Assays

All experimental procedures involving murine cells and human biological samples were conducted in accordance with national and international ethical guidelines. The study protocol was approved by the Research Ethics Committee (Comitê de Ética em Pesquisa—CEP) of São Paulo State University (UNESP), Faculty of Sciences and Letters, Assis Campus (FCL-Assis), Brazil, under approval number 12322010.

Human blood used in the HRBC assay was obtained from healthy adult volunteers after written informed consent and in accordance with the ethical standards of the Brazilian National Health Council Resolution 466/2012 and the Declaration of Helsinki. To ensure donor privacy, samples were anonymized prior to processing and only de-identified data were analyzed. No vulnerable populations were involved in this study.

2.8.1. Inhibition of Phagocytosis

Phagocytic activity was evaluated in murine RAW 264.7 macrophages as described in the literature, with adaptations for the use of nanomembrane eluates [5]. Macrophages were seeded in 24-well plates containing sterile coverslips at a density of 2×10^5 cells per well using high-glucose DMEM® supplemented with 10% fetal bovine serum (FBS) and incubated overnight at 37 °C in a humidified atmosphere containing 5% CO_2 to allow cell adhesion. After adhesion, cells were washed with PBS and subjected to the following treatments for 2 h: negative control (NC), consisting of DMEM supplemented with 0.9% saline solution and zymosan A; positive control (PC), containing dexamethasone at 40 µg/mL; and experimental groups treated with nanomembrane eluates (PCL and PCL+EAH 5%). The eluates were previously obtained by incubating the nanomembranes in supplemented DMEM containing 10% FBS, penicillin at 100 U/mL, and streptomycin at 100 µg/mL, at a surface-to-volume ratio of 3 cm^2/mL for 24 h at 37 °C.

After the treatment period, the coverslips were washed to remove non-internalized particles, and the cells were fixed in 2.5% glutaraldehyde for 10 min and stained with Wright's stain. Phagocytic activity was quantified by optical microscopy at 1000× magnification

by counting 100 cells per coverslip to determine the phagocytic index. The percentage of phagocytosis inhibition (PI) was calculated according to the following Equation (1):

$$PI(\%) = \frac{E_0 - E_t}{E_0} \times 100 \quad (1)$$

where E_0 corresponds to the mean value of the negative control group and E_t corresponds to the mean value of the treated groups.

2.8.2. Inhibition of Macrophage Spreading

Macrophage spreading was evaluated by a morphological adhesion and spreading assay with microscopic quantification, as described in the literature, with adaptations [5]. Cell suspensions were prepared at a concentration of 5.0×10^5 cells/mL in high-glucose DMEM® supplemented with 10% fetal bovine serum (FBS). Aliquots of 100 µL were distributed onto sterile coverslips placed in culture plates, allowing initial adhesion for 15 min at 25 °C.

After removal of non-adherent cells by washing with 0.9% saline solution, culture medium containing the following treatments was added: (i) negative control (NC), consisting of cells maintained only in culture medium; (ii) positive control (PC), consisting of dexamethasone at 40 µg/mL; and (iii) experimental groups treated with nanomembrane eluates (PCL and PCL+EAH 5%), previously prepared at a surface-to-volume ratio of 3 cm^2/mL by incubation at 37 °C for 24 h, as described in Section 2.8.1.

After incubation for a period previously standardized in the laboratory, the coverslips were fixed and analyzed by optical microscopy. For each experimental condition, 100 cells per coverslip were evaluated and classified as spread or non-spread according to previously established morphological criteria, including flattened cells, increased surface area, and the presence of cytoplasmic projections. The percentage of spreading inhibition (SI) was calculated using the following Equation (2):

$$SI(\%) = \frac{E_0 - E_t}{E_0} \times 100 \quad (2)$$

where E_0 corresponds to the mean number of spread cells in the negative control group and E_t corresponds to the mean number of spread cells in the treated groups.

2.8.3. Inhibition of Hemolysis

Erythrocyte membrane stabilization activity using human red blood cells (HRBCs) was evaluated according to the methodology described by Mizushima and Kobayashi (1968) [12], with adaptations. The experimental groups consisted of a negative control (NC), composed of 0.9% saline solution; a positive control (PC), containing dexamethasone at 40 µg/mL; and treated groups containing nanomembrane eluates (PCL and PCL+EAH 5%).

The eluates were previously prepared by incubating the nanomembranes in appropriate culture medium, as described in Section 2.7. Subsequently, the samples were incubated with a suspension of human erythrocytes under hemolysis-inducing conditions. After the incubation period, the samples were centrifuged, and the supernatant was collected for spectrophotometric analysis to indirectly quantify the released hemoglobin.

The percentage of protection against hemolysis was calculated using the following Equation (3):

$$Protection(\%) = \frac{E_0 - E_t}{E_0} \times 100 \quad (3)$$

where E_0 represents the mean absorbance of the negative control and E_t represents the mean absorbance of the treated groups.

2.8.4. Inhibition of Albumin Denaturation

Inhibition of protein denaturation was determined according to the method described by Mizushima and Kobayashi (1968) [12], with adaptations. The reaction mixture consisted of 0.05 mL of treatments, including negative control (NC), composed of 0.9% saline solution; positive control (PC), containing dexamethasone at 40 µg/mL; and eluates of PCL and PCL+EAH 5%, prepared in 10% (*v*/*v*) polyethylene glycol according to the laboratory protocol, combined with 0.45 mL of 5% (*w*/*v*) bovine serum albumin. The pH was adjusted to 6.3 using 0.1 N HCl, followed by incubation at 37 °C for 20 min and heating at 57 °C for 3 min. After cooling, 2.5 mL of phosphate-buffered saline (PBS, pH 6.3) was added, and turbidity was measured at 660 nm.

The percentage of protection against protein denaturation was calculated using the following Equation (4):

$$Protection(\%) = \frac{E_0 - E_t}{E_0} \times 100 \quad (4)$$

where E_0 represents the mean absorbance of the negative control and E_t represents the mean absorbance of the treated groups [12].

2.8.5. Cell Migration Assay

Pro-healing potential was evaluated using the in vitro wound closure assay (scratch assay), as described by Liang, Park, and Guan (2007) and Grada et al. (2017) [13,14], with adaptations. Murine NIH/3T3 fibroblasts (ATCC® CRL-1658™; American Type Culture Collection, Manassas, VA, USA) were cultured in high-glucose DMEM supplemented with 10% fetal bovine serum (FBS), penicillin at 100 µg/mL, and streptomycin at 100 µg/mL, and maintained at 37 °C in a humidified atmosphere containing 5% CO_2. Cells were seeded in 48-well plates until approximately 90% confluence was reached. A linear scratch, representing an artificial wound, was created using a sterile p200 pipette tip. Cellular debris was removed with PBS, and DMEM containing 2% FBS was added.

Treatments consisted of the application of nanomembrane eluates (PCL and PCL+EAH 5%), previously obtained by incubating the membranes in assay medium at 37 °C for 24 h at a surface-to-volume ratio of 3 cm^2/mL. The negative control (NC) consisted of exposure of cells to 0.9% saline solution under the same experimental conditions. Images were captured using optical microscopy at 0, 24, 48, and 72 h, as presented in the Results section, and the wound area was quantified using ImageJ software. Wound closure was expressed as a percentage according to the following Equation (5):

$$Wound\ \text{closure}(\%) = \frac{A_0 - A_t}{A_0} \times 100 \quad (5)$$

where A_0 corresponds to the initial wound area and A_t corresponds to the area measured at each experimental time point [13,14].

2.9. Statistical Analysis

All experiments were performed using three independent biological replicates (n = 3) (i.e., independent experiments performed on different days). For each biological replicate, measurements were acquired in technical triplicate whenever applicable. Data are presented as mean ± standard deviation (SD). Statistical analyses were conducted using Biostat 5.3 and GraphPad Prism 9.0 software. Comparisons among groups were performed by one-way ANOVA followed by Tukey's post hoc test. For time-course assays (e.g., MTT at 24, 48 and 72 h), one-way ANOVA was performed separately at each time point. Differences were considered statistically significant at $p < 0.05$. In the figures, different superscript

letters indicate statistically significant differences among groups (Tukey, $\alpha = 0.05$). Graphs were generated using GraphPad Prism.

3. Results

3.1. Phytochemical Screening of Saponins (EDP) and Sapogenins (EAH)

To better understand the pharmacological effects exhibited by EDP and EAH, phytochemical analyses were performed. Table 1 presents the results obtained from spectrophotometric analyses, expressed as g/100 g of dry extract, calculated as standard equivalents. Quantification was carried out using a spectrophotometric method with *Quillaja* saponins as the reference standard for total saponins, based on a linear calibration curve ($y = 0.0022x - 0.0039$; $R^2 = 0.9974$). For sapogenins, diosgenin was used as the reference standard, also with a linear calibration curve ($y = 0.0057x - 0.0117$; $R^2 = 0.9985$).

Table 1. Quantification of total saponins in EDP and total sapogenins in EAH, expressed as g/100 g of dry extract. Results are expressed as *Quillaja* saponin equivalents and diosgenin equivalents, respectively.

Sample	Content (g/100 g Dry Extract)
EDP (total saponins)	33.83 ± 2.93
EAH (total sapogenins)	11.56 ± 0.60

3.2. Fourier Transform Infrared Spectroscopy (FTIR) Analysis

Normalized spectra enabled direct comparison between the control sample (pure PCL) and the samples functionalized with 5% extracts (Figure 3). In all samples, the characteristic bands of poly(ε-caprolactone) (PCL) were preserved, notably: (i) C–H stretching vibrations of CH_2 groups at approximately 2945–2950 and 2850 cm^{-1}; (ii) the ester carbonyl (C=O) band at approximately 1720–1722 cm^{-1}; (iii) C–O and C–O–C vibrations in the region of approximately 1290–1240 cm^{-1}; and (iv) CH_2 rocking vibrations at approximately 730–725 cm^{-1}, associated with the crystalline fraction of PCL.

The preservation of these spectral signatures indicates structural integrity of the polymeric matrix after surface functionalization, with no spectroscopic evidence of degradation induced by the coating procedure. These findings are consistent with previously reported FTIR band assignments for electrospun PCL mats [15,16].

In PCL+EDP 5%, moderate changes were observed in the 1200–900 cm^{-1} region, with reinforcement of bands compatible with increased contribution of oxygenated groups, particularly C–O vibrations. This behavior is consistent with the presence of glycosylated saponin-rich fractions of plant origin, while preserving the dominant PCL bands. Such spectral features indicate predominantly superficial incorporation with comparatively lower relative intensity, which may reflect a reduced surface-associated contribution [17,18].

For PCL+EAH 5%, the spectral changes were more pronounced, including a broader O–H stretching contribution in the 3400–3530 cm^{-1} range and marked enhancement of signals in the 1300–700 cm^{-1} region. In particular, intensified bands at approximately 1262 cm^{-1} and 1019–1030 cm^{-1}, attributed to C–O and C–O–C vibrations, were observed, indicating a higher contribution of oxygenated species on the membrane surface. These results are consistent with the nature of the hydrolyzed extract (EAH), as the hydrolysis process may alter the saponin profile and enrich sapogenin-related fractions, favoring greater exposure of functional groups and more evident surface coverage detectable by FTIR-ATR [5,18].

Overall, the FTIR spectra indicate that both EDP and EAH were incorporated into the nanomembranes through physical interaction and surface coating mechanisms, preserving the integrity of the characteristic PCL bands, including the ester carbonyl (C=O) band. A

comparatively higher degree of surface functionalization was observed for PCL+EAH 5% relative to PCL+EDP 5% [16,18].

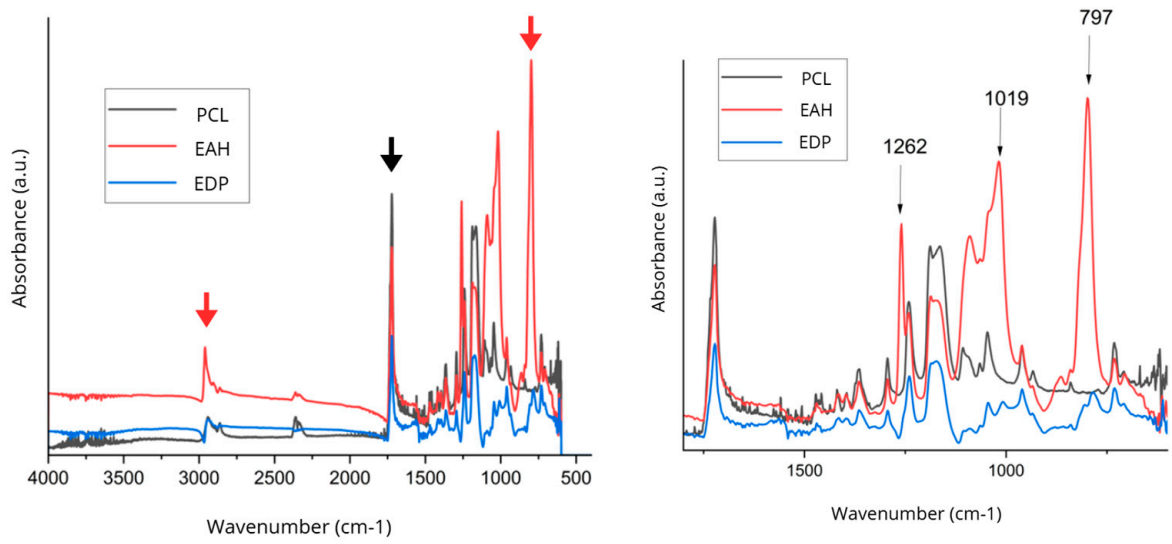

Figure 3. FTIR-ATR spectra of nanofibrous membranes: pure PCL (control), PCL+EDP 5%, and PCL+EAH 5%. The full-spectrum profiles (**left**) show preservation of the characteristic PCL bands, particularly the ester carbonyl stretch at approximately 1720 to 1722 cm^{-1} (C=O) and the CH_2 stretching bands at approximately 2945 and 2865 cm^{-1}, indicating that the post-electrospinning functionalization did not compromise the polymer backbone. The enlarged fingerprint region (**right**) highlights extract-dependent spectral contributions, with more pronounced intensity changes for PCL+EAH 5%, especially around 1262 and 1019 cm^{-1}, compared with PCL+EDP 5%, consistent with a greater contribution of oxygenated surface-associated constituents. Arrows indicate the main characteristic absorption bands discussed in the text. Overall, the spectra support predominantly physical surface incorporation of *Agave sisalana* fractions while maintaining the structural integrity of the PCL matrix.

3.3. Scanning Electron Microscopy (SEM)

Morphological characterization of the nanomembranes was performed by scanning electron microscopy (SEM; ZEISS EVO LS15, Carl Zeiss Microscopy, Oberkochen, Germany) for control PCL and for samples functionalized with EDP and EAH at concentrations of 1% and 5%, aiming to verify possible structural changes associated with extract type and increasing concentration.

Overall, the micrographs revealed fibrous mats composed of continuous, predominantly cylindrical fibers with no marked presence of beads, forming a random network typical of electrospun materials. In the functionalized samples (Figures 4 and 5), the main observed changes were related to the fiber diameter distribution profile, with increased heterogeneity, and the presence of locally thicker segments. These features are consistent with surface coating and deposition effects resulting from post-electrospinning functionalization by drop coating. Importantly, the functionalization step using hydroethanolic solutions did not promote fiber coalescence or collapse of the porous structure, preserving the characteristic fibrous architecture of electrospun membranes. This behavior is attributed to the fact that ethanol acts as a non-solvent for poly(ε-caprolactone).

Regarding fiber diameter, control PCL exhibited a mean diameter of 611 nm with a median of 583 nm. For EAH-functionalized samples, mean diameters of 680 nm (1%) and 748 nm (5%) were observed (Figure 4). Notably, the EAH 5% formulation showed a lower median diameter of 495 nm and higher dispersion, with a standard deviation of 631 nm and a diameter range of 102–2797 nm, suggesting the coexistence of a substantial population of thin fibers together with a fraction of thicker fibers that increases the mean value. For

EDP-functionalized samples, mean fiber diameters were 741 nm (1%) and 790 nm (5%), with increased variability at 5% concentration, reflected by a standard deviation of 506 nm (Figure 5). This trend is consistent with greater morphological heterogeneity at higher extract concentrations.

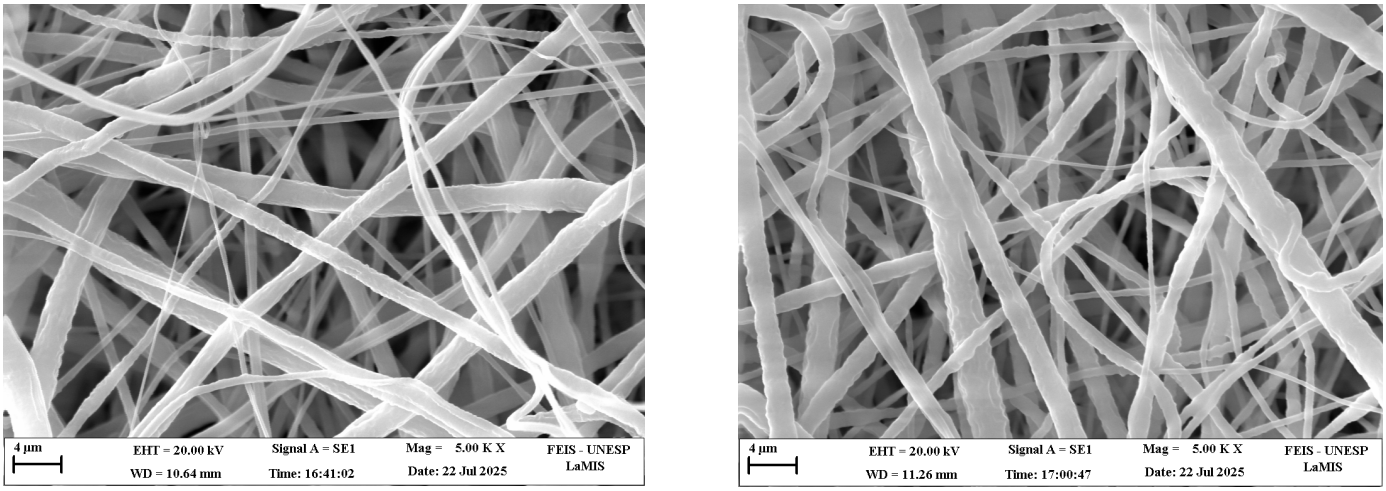

Figure 4. Scanning electron micrographs (SEMs) of electrospun PCL membranes functionalized with acid-hydrolyzed extract (EAH) from *Agave sisalana* (1% and 5%). The nanofibrous structure remained continuous and bead-free, supporting successful surface functionalization. Scale bar = 4 µm.

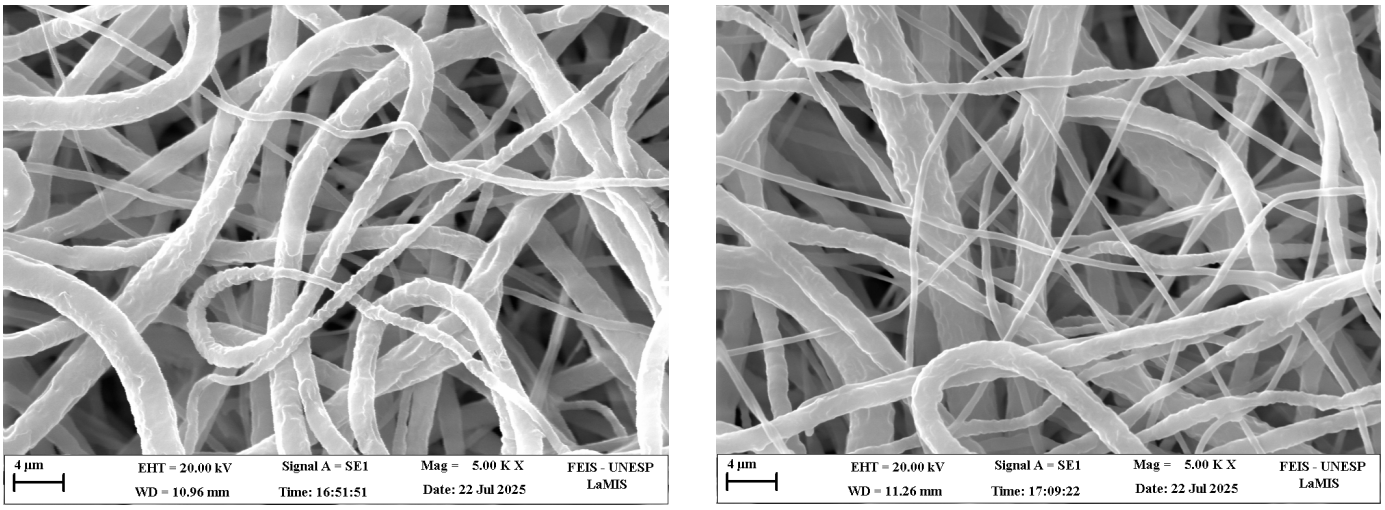

Figure 5. Scanning electron micrographs (SEMs) of electrospun PCL membranes functionalized with extract of the dry precipitate (EDP) from *Agave sisalana* (1% and 5%). Fibers remained continuous and predominantly bead-free, enabling comparative morphological assessment among formulations. Scale bar = 4 µm.

Taken together, these results indicate that functionalization with sisal-derived extracts affects not only the average fiber diameter but mainly the diameter distribution profile, while preserving the overall fibrous morphology and structural integrity of the nanomembrane under the evaluated conditions. The fiber diameter distribution profiles for all formulations are presented in Figure 6.

EDP-containing membranes exhibited slightly larger fiber diameters, which may be related to the amphiphilic nature of glycosylated saponins, potentially affecting surface interactions within the nanofibrous network. Despite these variations, all membranes preserved a porous and interconnected nanofibrous structure, indicating that the surface functionalization strategy maintained the structural integrity of the electrospun PCL fibers.

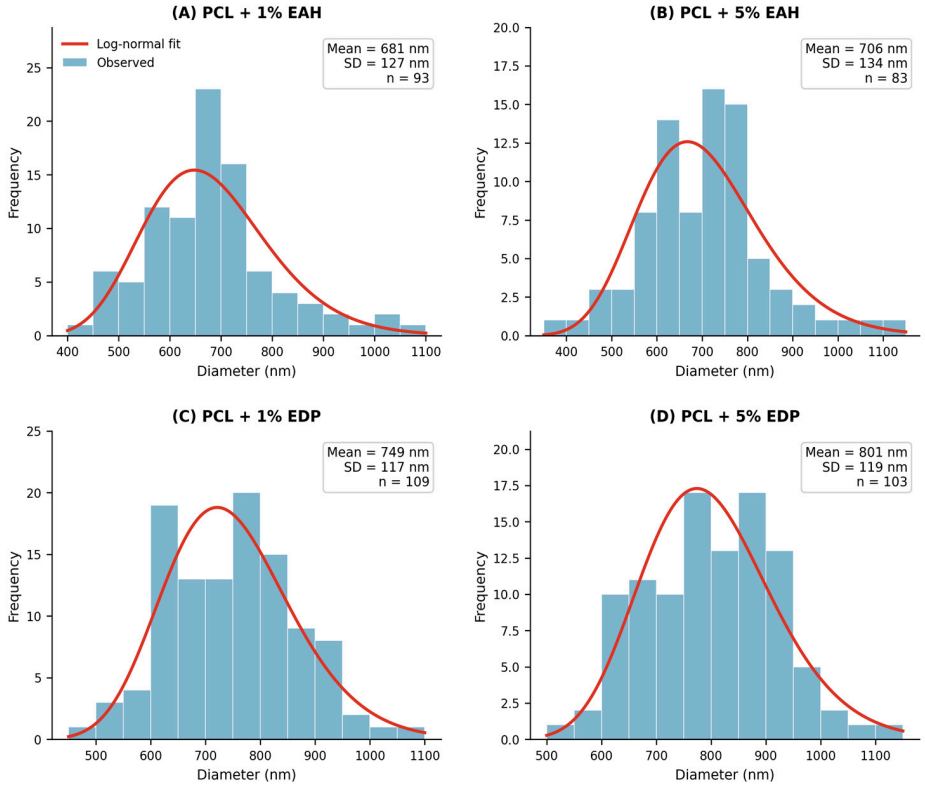

Figure 6. Fiber diameter distribution of electrospun PCL membranes functionalized with sisal-derived fractions. Fiber diameters were measured from SEM micrographs using ImageJ software ($n \approx 100$ fibers per sample). Red curves represent log-normal distribution fits applied to each histogram. (**A**) PCL+EAH 1%; (**B**) PCL+EAH 5%; (**C**) PCL+EDP 1%; (**D**) PCL+EDP 5%.

3.4. Cell Viability

Cell viability was determined using eluates obtained from nanomembranes containing EAH and EDP, employing NIH/3T3 fibroblasts subjected to the MTT assay. Figure 7 illustrates cell viability values (%) after 24, 48, and 72 h of exposure to the eluates. The positive control (PC) exhibited a pronounced cytotoxic effect at all evaluated time points, with a significant reduction in viability compared with the negative control ($p < 0.05$).

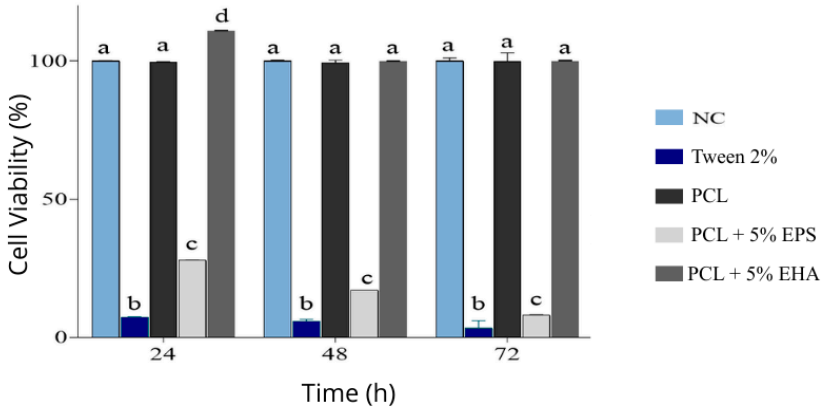

Figure 7. Mean ± SD of cell viability assessed by the MTT assay in NIH/3T3 fibroblasts after 24, 48, and 72 h of exposure to the treatments: NC, negative control or vehicle (0.9% saline solution in culture medium); PC, positive control (2% Tween 80 in culture medium); PCL, poly(ε-caprolactone) nanomembrane; and PCL+EDP 5% or PCL+EAH 5%. Statistical analysis: one-way ANOVA followed by Tukey's post hoc test performed separately at each time point. Different superscript letters indicate statistically significant differences among groups within the same time point ($\alpha = 0.05$). $n = 3$ independent biological replicates (with technical triplicates where applicable).

Treatment with PCL+EDP 5% resulted in a marked decrease in cell viability, with values of 28 ± 0.03% at 24 h, 17 ± 0.04% at 48 h, and 8 ± 0.20% at 72 h. These values differed statistically from both the negative and positive controls at all time points ($p < 0.05$). In contrast, PCL+EAH 5% showed significantly higher viability than the negative control only at 24 h, reaching 111 ± 0.03% ($p < 0.05$), while no statistically significant differences were observed at 48 h, with 100 ± 0.04%, or at 72 h, with 100 ± 0.02%, when compared with the negative control ($p > 0.05$).

Pure PCL maintained cell viability close to 100% at all analyzed time points, with values of 99.65 ± 0.15% at 24 h, 99.54 ± 0.78% at 48 h, and 100 ± 2.98% at 72 h. These results did not differ significantly from the negative control ($p > 0.05$), indicating the absence of cytotoxic effects. The visual appearance of formazan crystal formation for each treatment group is shown in Figure 8.

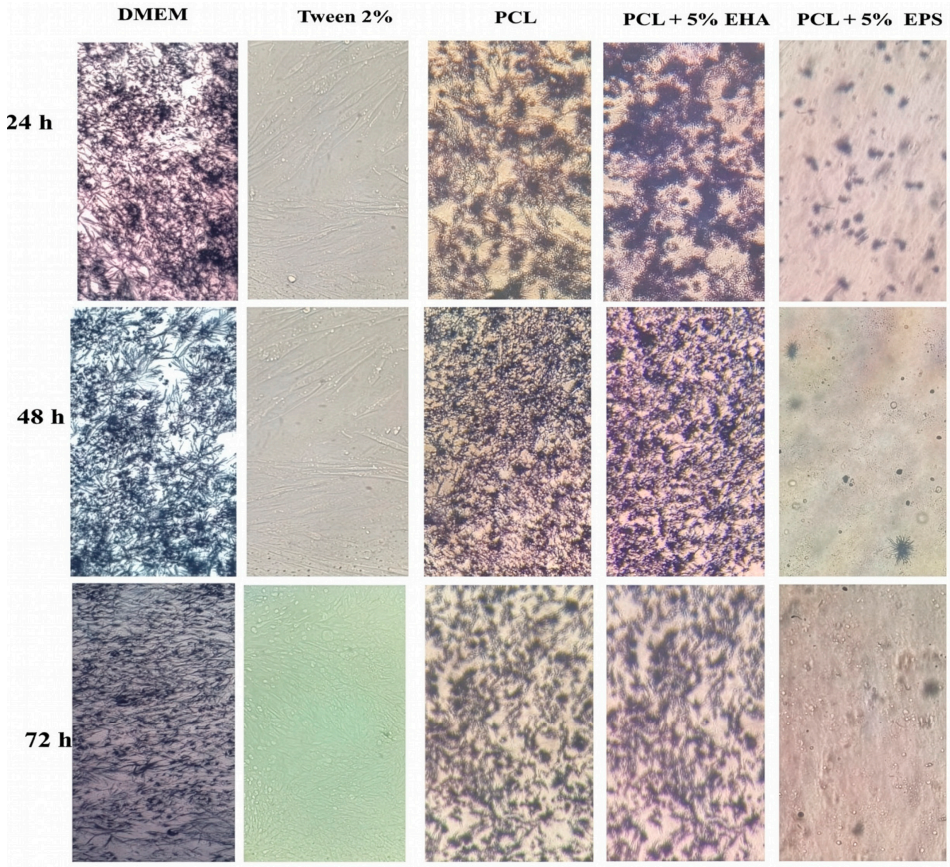

Figure 8. Visual appearance of formazan crystal formation at 24, 48, and 72 h after MTT addition in NIH/3T3 fibroblasts exposed to the following treatments: CB, unexposed cells; PCL, poly(ε-caprolactone) nanomembrane; and PCL+EDP 5% or PCL+EAH 5%. Images were acquired using a 20× objective lens on an inverted optical microscope and are presented as qualitative visual records of colorimetric differences among treatment groups.

3.5. Pharmacological Assays

3.5.1. Inhibition of Phagocytosis

Figure 9 illustrates the inhibition of phagocytosis observed for the different treatments. The negative control (NC; DMEM supplemented with 0.9% saline solution and zymosan A) exhibited a baseline value of 0.00 ± 0.00%, whereas the positive control (PC; dexamethasone at 40 µg/mL) showed 84.54 ± 3.86% inhibition. Treatment with the PCL eluate resulted in an inhibition value of 17.43 ± 5.23%, while the PCL+EAH 5% group exhibited 75.00 ± 3.53% inhibition. All treated groups differed significantly from the negative control ($p < 0.0001$).

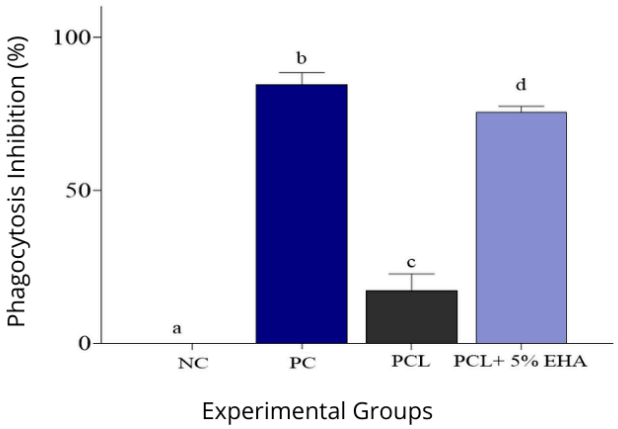

Figure 9. Mean ± SD of phagocytosis inhibition in murine macrophages after treatment with the following groups: NC, negative control (DMEM supplemented with 0.9% saline solution and zymosan A); PC, positive control (dexamethasone at 40 µg/mL); PCL, eluate from the poly(ε-caprolactone) nanomembrane; and PCL+EAH 5%, eluate. Statistical analysis was performed using one-way ANOVA followed by Tukey's post hoc test. Statistically significant differences ($p < 0.0001$) are indicated by different superscript letters; $n = 3$ independent biological replicates (with technical triplicates where applicable).

3.5.2. Inhibition of Macrophage Spreading

Figure 10 illustrates the results of the macrophage spreading inhibition assay for the different evaluated treatments. The negative control (NC) exhibited a baseline value of 0.00 ± 0.00%, whereas the positive control (PC; dexamethasone at 40 µg/mL) promoted pronounced inhibition of cell spreading, reaching 90.80 ± 3.05%. The PCL nanomembrane induced 22.99 ± 2.30% inhibition of spreading, while PCL+EAH 5% promoted an inhibition of 62.45 ± 1.35%, highlighting the ability of EAH to modulate the cellular response. All treated groups differed statistically from the negative control ($p < 0.0001$).

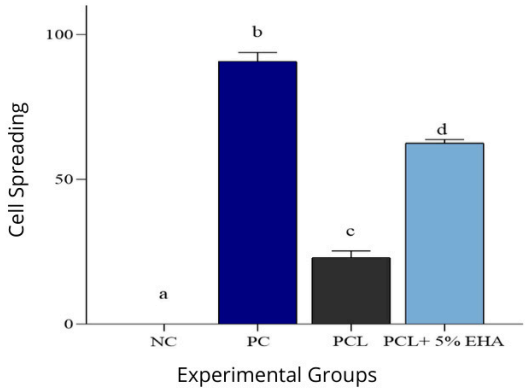

Figure 10. Mean ± SD of macrophage spreading inhibition for the following treatments: NC, negative control (0.9% saline solution); PC, positive control (dexamethasone at 40 µg/mL); PCL, poly(ε-caprolactone) nanomembrane; and PCL+EAH 5%. Statistical analysis was performed using one-way ANOVA followed by Tukey's post hoc test. Statistically significant differences ($p < 0.0001$) are indicated by different superscript letters; $n = 3$ independent biological replicates (with technical triplicates where applicable).

3.5.3. Inhibition of Hemolysis

Figure 11 illustrates the results of the erythrocyte membrane stabilization assay (HRBC), expressed as the percentage of protection against hemolysis relative to the negative control. The negative control (NC; 0.9% saline solution) exhibited a baseline value of 0.00 ± 0.00%, whereas the positive control (PC; dexamethasone at 40 µg/mL) showed

96.00 ± 0.05% protection. Treatment with the PCL eluate resulted in 12.31 ± 0.05% protection, while the PCL+EAH 5% group exhibited 56.00 ± 0.05% protection. All treated groups differed significantly from the negative control ($p < 0.0001$).

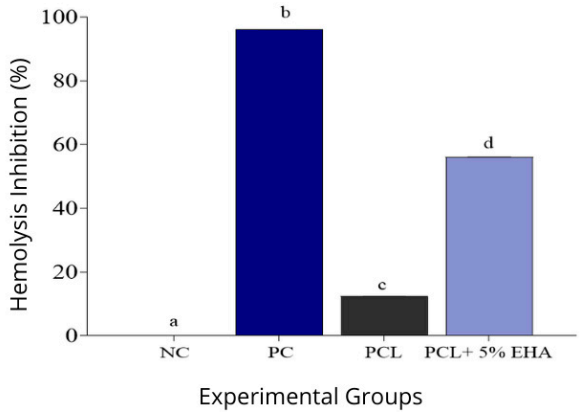

Figure 11. Mean ± SD of protection against hemolysis in the erythrocyte membrane stabilization assay (HRBC) for the following treatments: NC, negative control (0.9% saline solution); PC, positive control (dexamethasone at 40 µg/mL); PCL, eluate from the poly(ε-caprolactone) nanomembrane; and PCL+EAH 5%, eluate. Statistical analysis was performed using one-way ANOVA followed by Tukey's post hoc test. Statistically significant differences ($p < 0.0001$) are indicated by different superscript letters; $n = 3$ independent biological replicates (with technical triplicates where applicable).

3.5.4. Inhibition of Albumin Denaturation

Figure 12 presents the results obtained in the protein denaturation inhibition assay using albumin, expressed as percentages relative to the negative control. The negative control (NC) exhibited a baseline value of 0.00 ± 0.00%, whereas the positive control (PC; dexamethasone at 40 µg/mL) showed 30.00 ± 0.04% protection. Treatment with the PCL eluate resulted in 4.00 ± 0.05% protection, while the PCL+EAH 5% group exhibited 45.00 ± 0.05% protection. All treated groups differed significantly from the negative control ($p < 0.0001$).

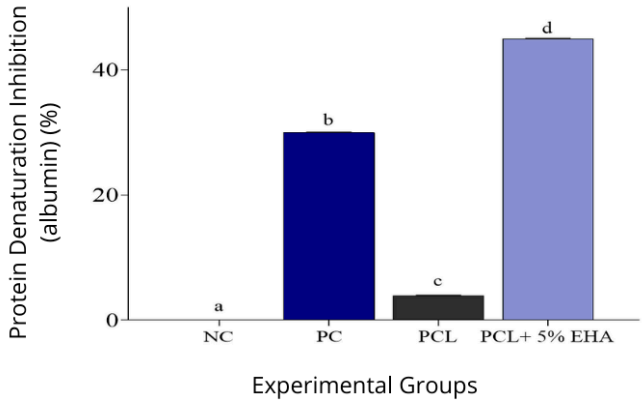

Figure 12. Mean ± SD of protection against protein denaturation using albumin for the following treatments: NC, negative control (0.9% saline solution); PC, positive control (dexamethasone at 40 µg/mL); PCL, eluate from the poly(ε-caprolactone) nanomembrane; and PCL+EAH 5%, eluate. Statistical analysis was performed using one-way ANOVA followed by Tukey's post hoc test. Statistically significant differences ($p < 0.0001$) are indicated by different superscript letters; $n = 3$ independent biological replicates (with technical triplicates where applicable).

3.6. Cell Migration

The pro-healing potential of the membranes was evaluated using the in vitro wound closure assay (scratch assay) in NIH/3T3 fibroblasts, as described by Liang et al. (2007)

and Grada et al. (2017) [13,14]. Figures 13 and 14 present, respectively, the quantification of wound area closure and representative visual images at 0, 24, 48, and 72 h.

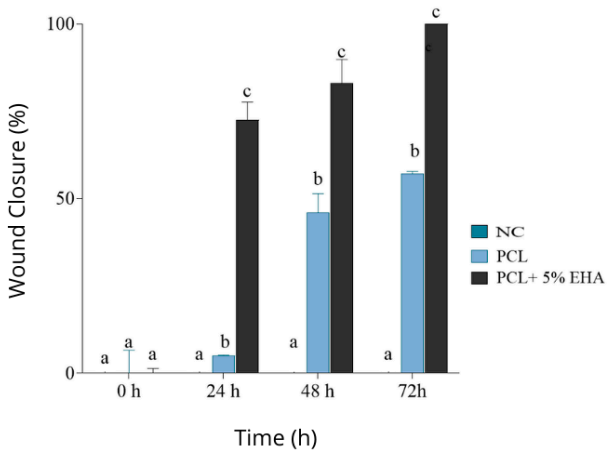

Figure 13. Mean ± SD of in vitro wound area closure assessed by the scratch assay for the following treatments: NC, negative control (0.9% saline solution); PCL, poly(ε-caprolactone) nanomembrane; and PCL+EAH 5%. Statistical analysis was performed using one-way ANOVA followed by Tukey's post hoc test. Statistically significant differences ($p < 0.05$) are indicated by different superscript letters; $n = 3$ independent biological replicates (with technical triplicates where applicable).

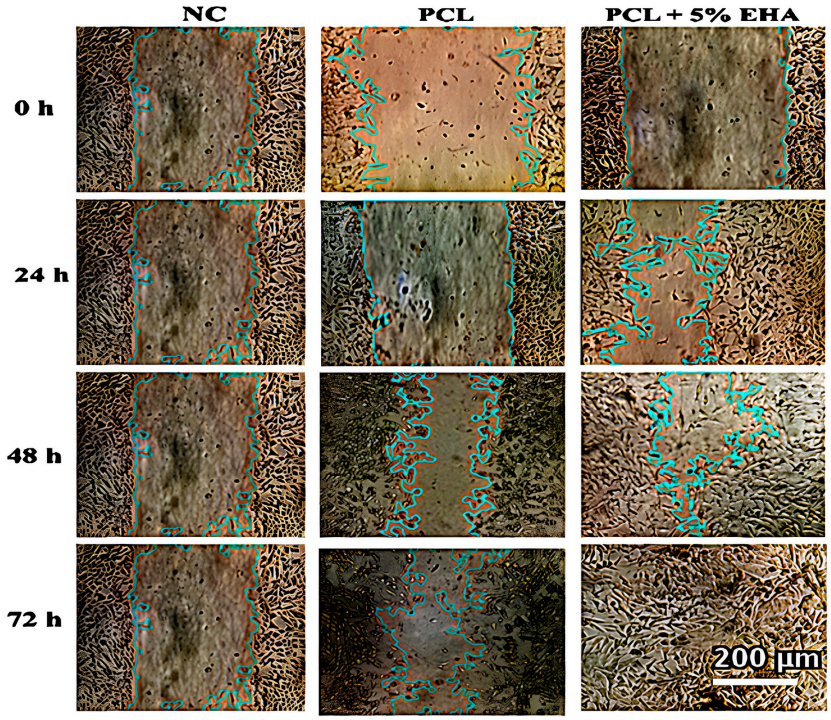

Figure 14. Representative images of the scratch assay showing wound closure at 0, 24, 48, and 72 h for NC (0.9% saline solution), PCL, and PCL+EAH 5%. Colored lines (cyan and red) indicate wound boundaries determined using ImageJ analysis. Scale bar = 200 µm.

The negative control (NC) showed no wound closure at any of the evaluated time points, with values of 0.00 ± 0.00%. The PCL membrane promoted moderate and progressive wound closure, reaching 5.00 ± 0.21% at 24 h, 46.00 ± 5.73% at 48 h, and 57.00 ± 0.70% at 72 h, differing significantly from the negative control ($p < 0.05$). The PCL+EAH 5% formulation exhibited superior performance, with wound closure values of 72.59 ± 5.83% at 24 h, 83.00 ± 6.80% at 48 h, and complete closure of 100.00 ± 0.00% at

72 h, indicating enhanced wound healing potential and statistically significant differences compared with the negative control ($p < 0.05$).

4. Discussion

This study was designed as a proof-of-concept of post-electrospinning surface functionalization, and therefore, several parameters relevant for advanced wound-dressing translation were not addressed here. First, the surface-deposited extracts were evaluated through standardized eluates and short-term biological readouts; quantitative loading efficiency and release kinetics were not measured because the approach aimed at surface modification rather than a controlled-release system. Second, additional physical and functional properties that are important for dressings—such as tensile strength/elongation, porosity/pore-size distribution, water vapor transmission rate (WVTR) and swelling/absorption capacity—were not evaluated in this phase. Finally, the biological assessment was limited to in vitro assays, and in vivo efficacy and safety will need to be investigated in future studies. Addressing these aspects will be part of the next development stage of the PCL+EAH platform.

Chronic wounds represent a significant public health problem, directly affecting patients' quality of life and generating high costs for healthcare systems due to inadequate and prolonged healing processes [19]. The difficulty in resolving these lesions is often associated with persistent inflammatory processes that impair the transition between the phases of wound healing, namely inflammation, proliferation, and remodeling, as well as dysfunctions in immune and vascular responses [20]. The management of chronic wounds therefore remains challenging, since conventional dressings such as hydrocolloids, alginates, and foams frequently fail to promote adequate cellular regeneration or to effectively control inflammation, leading to delayed healing and an increased risk of complications, including infection and wound recurrence [20].

In contrast, poly(ε-caprolactone) (PCL) nanomembranes have emerged as a biocompatible biomaterial for the treatment of chronic wounds. This is mainly attributed to their continuous and porous fibrous architecture, combined with high surface area, which mimics the extracellular matrix and enables more effective cell–material interactions [2,3,9]. In addition, functionalization of PCL nanomembranes with plant-derived extracts may enable local availability of surface-associated bioactive compounds and modulation of inflammatory responses, which are key factors in regulating cellular behavior during tissue repair [4,5].

It is well established that the liquid fraction of *Agave sisalana* residue, namely sisal juice, is rich in saponins and sapogenins, which are bioactive compounds with therapeutic potential for the treatment of chronic wounds [11,17,21]. Saponins are known to modulate inflammatory responses by reducing the activation of M1 macrophages, which are responsible for chronic inflammation and the sustained release of pro-inflammatory mediators [5,21]. This modulation favors the transition toward the M2 macrophage phenotype, which plays a crucial role in tissue repair processes and inflammation resolution, thereby accelerating wound healing [5,21]. In addition, saponins exhibit antimicrobial activity [4,5,11], contributing to the control of bacterial infections that are frequently associated with chronic wounds. In this context, *Agave sisalana* extracts may assist in reducing inflammation and preventing infection, creating a microenvironment more favorable to cellular regeneration and faster healing [4,5,11,21].

Within this framework, the present study aimed to develop PCL nanomembranes incorporating *Agave sisalana* extracts and to evaluate their in vitro safety and pharmacological activity. Accordingly, the first stage of this study consisted of quantifying saponins in the EDP by UV-Vis spectrophotometry using the vanillin–sulfuric acid method. EDP exhibited a total saponin content of 33.83 ± 2.93 g per 100 g of dry extract. In another

study, Silva Filho [22] reported a total saponin content of 17.8% in an extract obtained from the agroindustrial residue of *Agave sisalana*, supporting the significant presence of these bioactive compounds in the plant matrix and reinforcing the potential valorization of this residue as a natural source of saponins. Subsequently, sapogenins in the EAH were quantified by UV-Vis spectrophotometry using the anisaldehyde–sulfuric acid method, yielding a content of 11.56 ± 0.60 g per 100 g of diosgenin equivalents. These results confirm the efficiency of the hydrolysis process in releasing steroidal aglycones and justify their subsequent pharmacological evaluation. Phytochemical studies indicate that the main steroidal sapogenins present in *Agave sisalana* are hecogenin and tigogenin, which are aglycones derived from sisal saponins and are widely associated with anti-inflammatory activities [21].

After confirming the presence of saponins and sapogenins in the sisal extracts, respectively in EDP and EAH, the chemical and structural characterization of control PCL and the 5% functionalized nanomembranes was performed by FTIR-ATR. The results showed preservation of the dominant polymer bands, particularly the ester carbonyl (C=O) at approximately 1720 cm^{-1}, concomitant with intensification of signals in the fingerprint region associated with oxygenated groups (C–O and C–O–C) and O–H contribution in the 3400–3530 cm^{-1} range, more evident for the EAH formulation (Figure 3). The absence of new bands or systematic shifts compatible with the formation of covalent bonds detectable by FTIR-ATR suggests that incorporation occurred predominantly through physical interaction and surface coating, which is desirable for functional wound dressings. This interaction preserves polymer integrity and may favor bioactive availability in the wound microenvironment [2,3]. The more pronounced signature observed for EAH is consistent with fractions presenting a greater contribution of functional groups detectable by ATR, suggesting a more effective surface coverage.

Subsequently, morphological analysis by scanning electron microscopy (SEM) was used to evaluate the effect of functionalization on the architecture of the electrospun nanomembranes. The images indicated preservation of the continuous fibrous morphology and the characteristic porosity of PCL, with no evidence of structural collapse or significant fiber fusion after EAH incorporation. These findings are consistent with previous studies showing that maintaining fibrous topography is a determining factor for cell–material interactions and for the performance of electrospun dressings when compared with conventional formulations [2,3]. In addition, preservation of morphology and porosity after functionalization confirms that the post-processing step did not compromise platform integrity, supporting PCL as a robust base for the surface incorporation of natural bioactives. These findings support the potential of functionalized PCL nanomembranes as promising bioactive platforms for wound-related applications [3].

In this study, electrospun poly(ε-caprolactone) nanomembranes functionalized with extracts from *Agave sisalana* residue were evaluated as an alternative to conventional dressings such as hydrocolloids. Although hydrocolloids form a semi-occlusive layer that maintains a moist environment and facilitates healing, they present limitations in controlling inflammation and modulating critical cellular processes such as cell adhesion and migration. In addition, conventional dressings may be ineffective for wounds with high exudate or for chronic wounds, particularly in cases involving bacterial biofilms, which are common in patients with diabetes or venous insufficiency.

For cytotoxicity profiling, NIH/3T3 fibroblasts were used, since these connective tissue cells play an important role in chronic wound healing. When activated, fibroblasts are responsible for extracellular matrix synthesis, tissue remodeling, inflammation regulation, and facilitate angiogenesis and collagen formation, which are fundamental processes for repairing injured tissue. In vitro analyses such as the MTT cell viability assay are widely

applied to evaluate cytotoxicity and biological effects of substances on specific cells such as fibroblasts. The MTT method is based on the reduction of tetrazolium salt to formazan by viable mitochondria, providing a measure of cellular metabolic activity that reflects cell viability. Accordingly, in this study, the MTT assay was used to evaluate the cytotoxic effects of PCL, PCL+EDP 5%, and PCL+EAH 5%. The results indicated that only PCL+EDP 5% induced cytotoxicity (Figures 7 and 8). Based on these findings, the study proceeded exclusively with PCL and EAH 5% for subsequent pharmacological evaluations.

The extract-dependent cytotoxicity observed for PCL+EDP 5% can be mechanistically interpreted considering the chemical nature of glycosylated saponins. Due to their amphiphilic structure—comprising a hydrophobic steroidal nucleus linked to hydrophilic sugar chains—saponins may behave as natural surfactants, interacting strongly with lipid bilayers and increasing membrane permeability. At higher concentrations, this detergent-like behavior has been associated with membrane destabilization and loss of cellular integrity, which is consistent with the progressive reduction in fibroblast viability observed for EDP over 24–72 h. In contrast, the acid hydrolysis route used to obtain EAH favors the enrichment of sapogenins, which lack the glycosidic moieties that intensify amphiphilicity and membrane-disruptive effects. The reduced polarity of sapogenins may therefore contribute to improved cytocompatibility while preserving the steroidal scaffold associated with anti-inflammatory modulation, helping to explain why PCL+EAH 5% maintained viability and was suitable for subsequent pharmacological evaluation. Collectively, these findings reinforce that the biological performance of surface-functionalized nanofibrous systems is critically dependent not only on the botanical source but also on the phytochemical profile and degree of glycosylation of the incorporated fractions.

Inflammation in chronic wounds results from a dysregulated physiological process in which a persistent inflammatory response prevents the appropriate transition to the proliferation and remodeling phases of healing. Under normal conditions, inflammation is a necessary early response for defense against infection and cellular repair, mediated by cells such as neutrophils and macrophages, which perform phagocytosis of pathogens and cellular debris. However, in chronic wounds, this inflammatory phase is prolonged due to dysfunction in inflammatory mediators and persistence of M1 macrophages, which continue to release pro-inflammatory cytokines and impair inflammation resolution. This cycle of continuous inflammation prevents progression through healing phases, favoring chronic ulcer formation, infection, and failure of wound closure. Appropriate control of inflammation, including modulation of phagocytosis, is therefore important to accelerate healing and promote effective lesion resolution.

In this study, inhibition of phagocytosis in RAW 264.7 macrophages promoted by PCL treatment was 17.43 $\pm$ 5.23%. For PCL+EAH 5%, inhibition reached 75.00 $\pm$ 3.53%. The pronounced phagocytosis inhibition observed for PCL+EAH 5% is comparable to that described for other systems based on plant extracts rich in secondary metabolites, which are recognized for modulating macrophage activity and attenuating exacerbated inflammatory responses. Several studies demonstrate that plant-derived extracts and their bioactive compounds can directly interfere with macrophage phagocytosis and inflammatory activation through regulation of intracellular signaling pathways, contributing to inflammation resolution [5,21].

Macrophage spreading was subsequently evaluated. Spreading is part of the migration mechanism of these cells toward the lesion site, mediated by chemotactic signals such as cytokines and chemokines that are expressed at high levels in chronic wounds. These molecules signal macrophage recruitment to the inflammatory focus, promoting spreading and movement of immune cells to the wound site. This process occurs before phagocytosis and contributes to tissue restoration and modulation of inflammatory response. However,

in chronic inflammation, there is an immune imbalance and impaired healing, which favors chronic ulcer formation and prolongs the inflammatory process.

In the spreading inhibition assay, PCL promoted 22.99 ± 2.30% inhibition, whereas PCL+EAH 5% inhibited spreading by 62.45 ± 1.35%. The higher spreading inhibition observed for PCL+EAH 5% indicates more efficient modulation of macrophage activation and migration, processes that are closely related to the progression and maintenance of inflammation in chronic wounds. Previous studies demonstrate that plant extracts rich in secondary metabolites can interfere with cytoskeleton reorganization and macrophage intracellular signaling, reducing spreading and contributing to attenuation of inflammatory response [5,21].

Although phenotypic polarization markers were not directly evaluated in this study, the observed reduction in phagocytic activity and macrophage spreading suggests a modulatory effect on inflammatory activation. Persistent M1-type macrophage activity is a hallmark of chronic inflammatory environments, whereas attenuation of excessive activation is associated with progression toward resolution phases of tissue repair. In this context, the anti-inflammatory profile observed for PCL+EAH 5% may indicate a shift toward a more regulated inflammatory response, consistent with the known immunomodulatory potential of steroidal sapogenins. These findings support the hypothesis that selective enrichment of sapogenin fractions may contribute to balanced macrophage activity without compromising cellular viability.

Another in vitro method used to evaluate the anti-inflammatory activity of PCL and PCL+EAH 5% was the erythrocyte membrane stabilization test. Anti-inflammatory drugs can act by stabilizing lysosomal membranes, blocking the efflux of enzymes and their byproducts as well as physiological processes responsible for inflammatory amplification. Since erythrocyte and lysosomal membranes share similarities, stabilization of the erythrocyte membrane by PCL and PCL+EAH 5% suggests that this fraction may also be capable of stabilizing lysosomal membranes.

Protein denaturation inhibition is also a method frequently used to identify substances with anti-inflammatory activity without the need for animal models. This process is directly involved in the genesis of inflammation, since in vivo denaturation of tissue proteins compromises their biological function and favors persistent inflammatory responses, intensifying chronic wound development [20]. In this context, sapogenins stand out as safe sources of bioactive compounds with potential application as anti-inflammatory agents, complementing oral and/or topical non-steroidal anti-inflammatory drugs [5,21]. The low inhibition observed for PCL eluate alone (4.00 ± 0.05%) supports a limited capacity for protein structural protection, whereas PCL+EAH 5% exhibited significantly higher inhibition (45.00 ± 0.05%), suggesting that the sapogenin-enriched fraction contributes to attenuation of protein denaturation-associated inflammatory responses.

Finally, this study performed a two-dimensional in vitro cell migration assay, which can be conducted using primary skin cells such as keratinocytes, endothelial cells, and fibroblasts. This method is an essential tool in preclinical wound research, allowing investigation of mechanisms regulating cell migration and the effects of different experimental conditions on this process. The results indicated that treatment with PCL and particularly with PCL+EAH 5% significantly increased fibroblast migration rate compared with the control after 48 and 72 h of treatment ($p < 0.05$) (Figures 13 and 14). In addition, the wound treated with PCL+EAH 5% showed complete closure after 72 h, indicating enhanced pro-migratory activity under in vitro conditions.

Similar results have been reported for electrospun nanomembranes loaded with plant extracts, in which the combination of biomimetic nanofibrous architecture and local release of bioactive compounds promotes increased fibroblast migration and accelerates in vitro

wound closure [23,24]. Studies using PCL nanofibers or analogous polymeric systems loaded with botanical extracts reported near-complete scratch closure within 48 to 72 h, attributed to modulation of inflammatory response, stimulation of cell migration, and improved cell–material interactions [23,24].

Although quantitative loading efficiency and detailed release kinetics were not investigated in the present study, the eluate-based biological assays confirm that bioactive constituents associated with the membrane surface remain biologically available under physiological conditions. The functionalization strategy adopted here was designed as a surface modification approach rather than a controlled drug-delivery system, aiming primarily to evaluate extract-dependent biological modulation while preserving the structural integrity of the electrospun platform. Therefore, this study represents an initial validation of biological feasibility. Future investigations focusing on quantitative surface loading, release profiling, and long-term coating stability will be important to support further technological development and subsequent translational studies.

In summary, the results obtained in this study support the in vitro biological feasibility of surface-functionalized PCL nanomembranes enriched with sapogenin fractions derived from *Agave sisalana* residue. The extract-dependent responses observed throughout the physicochemical and biological evaluations reinforce the critical role of phytochemical composition in determining cytocompatibility and immunomodulatory behavior of electrospun platforms. Beyond the biological findings, this work also highlights a sustainable strategy for valorizing agroindustrial residues by converting underutilized biomass into functionally relevant bioactive modifiers. These findings provide a foundation for subsequent investigations aimed at advancing the technological maturation and translational exploration of sapogenin-enriched surface-functionalized systems.

5. Conclusions

This study demonstrated the feasibility of producing electrospun poly(ε-caprolactone) (PCL) nanomembranes and functionalizing them by drop coating with extracts derived from *Agave sisalana*, while preserving the nanofibrous architecture required for application in functional wound dressings. FTIR-ATR analysis confirmed the chemical integrity of PCL after functionalization and indicated a predominantly physical incorporation of oxygenated constituents from the extracts, with a more pronounced spectral signature for EAH 5%, suggesting a more effective surface coating.

Phytochemical quantification revealed a high concentration of total saponins in EDP (33.83 ± 2.93 g/100 g) and total sapogenins in EAH (11.56 ± 0.60 g/100 g). However, in the MTT assay, PCL+EDP 5% induced cytotoxicity. In contrast, in vitro pharmacological evaluations demonstrated that PCL+EAH 5% exhibited results indicative of anti-inflammatory activity and pro-healing potential.

As a next step toward the development of a novel bioactive wound dressing based on PCL+EAH 5% nanomembranes, the following are required: (i) chemical standardization using specific markers such as hecogenin and tigogenin; (ii) evaluation of coating stability and release kinetics; (iii) assessment of performance parameters relevant to wound dressings, including mechanical properties, barrier function, and exudate management, to strengthen reproducibility and technological maturation; and (iv) in vivo studies to confirm the pharmacological activities observed in vitro.

Author Contributions: Conceptualization, F.R.Z.L.N. and L.d.S.; methodology, J.A.R.F., W.R.P.M. and L.M.M.C.; software, L.T.S.d.C.; writing—original draft preparation, F.R.Z.L.N., J.A.R.F. and A.L.S.C.; visualization, L.d.S.; project administration, L.d.S. All authors have read and agreed to the published version of the manuscript.

Funding: The authors thank the Coordination for the Improvement of Higher Education Personnel (CAPES—Brazil) for the doctoral scholarships (Process No. 888 87.827298/2023-00).

Institutional Review Board Statement: Not applicable.

Informed Consent Statement: Not applicable.

Data Availability Statement: All data are contained in this article.

Acknowledgments: During the preparation of this manuscript, the authors used ChatGPT 5.1 and Gemini 3 for language editing and translation improvement. The authors carefully reviewed and edited the generated text and take full responsibility for the content of this publication.

Conflicts of Interest: The authors declare no conflicts of interest.

Abbreviations

The following abbreviations are used in this manuscript:

ATR	Attenuated Total Reflectance
CB	Unexposed control cells (blank)
DMEM	Dulbecco's Modified Eagle Medium
EAH	Acid-hydrolyzed extract
EDP	Extract of the dried precipitate
FTIR	Fourier Transform Infrared Spectroscopy
HRBC	Human red blood cell membrane stabilization assay
MTT	3-(4,5-dimethylthiazol-2-yl)-2,5-diphenyltetrazolium bromide
NC	Negative control
PBS	Phosphate-buffered saline
PC	Positive control
PCL	Poly(ε-caprolactone)
SEM	Scanning Electron Microscopy
UV–Vis	Ultraviolet–visible spectroscopy

References

1. Fleury, S.I.P.; Santos, A.G.; Gallo, S.T.; Nogueira, P.C. Cultural adaptation of the "Wounds at Risk Score" instrument for Brazilian Portuguese. In *Proceedings of the SOBEST Research and Extension Congress*; SOBEST: São Paulo, Brazil, 2023. Available online: https://anais.sobest.com.br/cpe/article/view/1100 (accessed on 5 January 2026).
2. Mafaldo, C.F.; Pereira, C.R.; Zinhani, M.C.; Backes, D.S.; Sagrillo, M.R.; Rodrigues Junior, L.F. Nanotechnology in smart dressings: Advances in the wound healing process—A systematic review. *Discip. Sci. Nat. Technol. Sci.* **2025**, *25*, 131–144. [CrossRef]
3. Silva, H.S.; Gonzales, K.R.S.; Freitas, J.D.; Lopes, A.C.O.; Carmo, D.R.; de Paula, F.R.; Costa, L.M.M. Production of electrospun poly(ε-caprolactone) mats containing brown propolis extract. *Cad. Pedagog. (Noteb. Pedagog.)* **2022**, *22*, e15674. [CrossRef]
4. Fracasso, J.A.R.; Takahashi, M.E.; Costa, L.T.S.; Barbosa, R.M.; Guarnier, L.P.; Almeida, L.T.; Santos, L. Development of a topical cream from the ethanolic extract of *Agave sisalana* residues with anti-inflammatory and analgesic properties. *Cosmetics* **2024**, *11*, 180. [CrossRef]
5. Costa, L.T.S.; Fracasso, J.A.R.; Guarnier, L.P.; Lima, S.C.; Paiva, P.B.; Miranda, L.M.; de Almeida, L.T.; Santos, L. Toxicity and anti-inflammatory effects of *Agave sisalana* extract derived from agroindustrial residue. *Plants* **2023**, *12*, 1523. [CrossRef] [PubMed]
6. Fracasso, J.A.R.; Sikina, I.Y.G.; Costa, L.T.S.; Guarnier, L.P.; Ribeiro-Paes, J.T.; Ferreira, F.Y.; Almeida, L.V.C.; Castro Silva, B.; Barbosa, D.B.; Ximenes, V.F.; et al. Toxicological profile and anti-inflammatory effect of mucoadhesive gel from residues of *Agave sisalana* and *Punica granatum*. *Gels* **2023**, *9*, 942. [CrossRef]
7. Wang, Y.; Ma, Y.; Tao, L.; Zhang, X.; Hao, F.; Zhao, S.; Han, L.; Liu, T. Recent advances in separation and analysis of saponins in natural products. *Separations* **2022**, *9*, 163. [CrossRef]
8. Baccou, J.C.; Lambert, F.; Sauvaire, Y. Spectrophotometric method for the determination of total steroidal sapogenin. *Analyst* **1977**, *102*, 458–465. [CrossRef] [PubMed]
9. Mercante, L.A.; Corrêa, D.S. (Eds.) *Electrospinning and Nanofibers: Fundamentals and Applications*; Atena: Ponta Grossa, Brazil, 2023. [CrossRef]
10. Schneider, C.A.; Rasband, W.S.; Eliceiri, K.W. NIH Image to ImageJ: 25 years of image analysis. *Nat. Methods* **2012**, *9*, 671–675. [CrossRef]

11. Araldi, R.P.; dos Santos, M.O.; Barbon, F.F.; Manjerona, B.A.; Meirelles, B.R.; de Oliva Neto, P.; da Silva, P.I.; dos Santos, L.; Camargo, I.C.C.; de Souza, E.B. Analysis of antioxidant, cytotoxic and mutagenic potential of *Agave sisalana* extracts. *Biomed. Pharmacother.* **2018**, *106*, 1161–1170. [CrossRef]
12. Mizushima, Y.; Kobayashi, M. Interaction of anti-inflammatory drugs with serum proteins, especially with some biologically active proteins. *J. Pharm. Pharmacol.* **1968**, *20*, 169–173. [CrossRef]
13. Liang, C.C.; Park, A.Y.; Guan, J.L. In vitro scratch assay: A convenient and inexpensive method for analysis of cell migration in vitro. *Nat. Protoc.* **2007**, *2*, 329–333. [CrossRef] [PubMed]
14. Grada, A.; Otero-Viñas, M.; Prieto-Castrillo, F.; Obagi, Z.; Falanga, V. Research techniques made simple: Analysis of collective cell migration using the wound scratch assay. *J. Investig. Dermatol.* **2017**, *137*, e11–e16. [CrossRef]
15. Persenaire, O.; Alexandre, M.; Degée, P.; Dubois, P. Mechanisms and kinetics of thermal degradation of poly(ε-caprolactone). *Biomacromolecules* **2001**, *2*, 288–294. [CrossRef]
16. de Almeida Cantalice, J.D.; Mazzini Júnior, E.G.; de Freitas, J.D.; da Silva, R.C.; Faez, R.; Costa, L.M.M.; Ribeiro, A.S. Polyaniline-based electrospun polycaprolactone nanofibers: Preparation and characterization. *Polym. Sci. Technol.* **2021**, *31*, e2021002. [CrossRef]
17. Ribeiro, B.D.; Coelho, M.A.Z.; Marrucho, I.M. Extraction of saponins from sisal (*Agave sisalana*) and juá (*Ziziphus joazeiro*) with cholinium-based ionic liquids and deep eutectic solvents. *Eur. Food Res. Technol.* **2013**, *237*, 965–975. [CrossRef]
18. Almutairi, M.S.; Ali, M. Direct detection of saponins in crude extracts of soapnuts by FTIR. *Nat. Prod. Res.* **2015**, *29*, 1271–1275. [CrossRef]
19. Martinengo, L.; Olsson, M.; Bajpai, R.; Soljak, M.; Upton, Z.; Schmidtchen, A.; Car, J.; Järbrink, K. Prevalence of chronic wounds in the general population: Systematic review and meta-analysis of observational studies. *Ann. Epidemiol.* **2019**, *29*, 8–15. [CrossRef] [PubMed]
20. Qian, L.-W.; Fourcaudot, A.B.; Yamane, K.; You, T.; Chan, R.K.; Leung, K.P. Exacerbated and prolonged inflammation impairs wound healing and increases scarring. *Wound Repair Regen.* **2016**, *24*, 26–34. [CrossRef] [PubMed]
21. Ingawale, D.K. Saponins and sapogenins of *Agave* with respect to diverse pharmacological role of hecogenin. *Int. J. Pharm. Pharm. Sci.* **2020**, *12*, 1–7. [CrossRef]
22. Silva Filho, J.A.A. Obtaining a Saponin-Rich Extract from *Agave sisalana* Industrial Residue for Application in the Cosmetic Industry. Master's Thesis, Federal University of Rio Grande do Norte, Natal, Brazil, 2022. Available online: https://repositorio.ufrn.br/server/api/core/bitstreams/d45d884e-7e68-4198-843f-66deeb747200/content (accessed on 5 January 2026).
23. Doostan, M.; Doostan, M.; Maleki, H.; Faridi Majidi, R.; Bagheri, F.; Ghanbari, H. Co-electrospun poly(vinyl alcohol)/poly(ε-caprolactone) nanofiber scaffolds containing coffee and *Calendula officinalis* extracts for wound healing applications. *J. Bioact. Compat. Polym.* **2022**, *37*, 437–452. [CrossRef]
24. Borges-Vilches, J.; Unalan, I.; Fernández, K.; Boccaccini, A.R. Fabrication of biocompatible electrospun poly(ε-caprolactone)/gelatin nanofibers loaded with *Pinus radiata* bark extracts for wound healing applications. *Polymers* **2022**, *14*, 2331. [CrossRef] [PubMed]